

Arteriosclerosis, Thrombosis, and Vascular Biology



JOURNAL OF THE AMERICAN HEART ASSOCIATION

Heparan Sulfate Proteoglycans Mediate the Angiogenic Activity of the Vascular Endothelial Growth Factor Receptor-2 Agonist Gremlin

Paola Chiodelli, Stefania Mitola, Cosetta Ravelli, Pasqua Oreste, Marco Rusnati and Marco Presta

Arterioscler Thromb Vasc Biol. 2011;31:e116-e127; originally published online September 15, 2011;

doi: 10.1161/ATVBAHA.111.235184

Arteriosclerosis, Thrombosis, and Vascular Biology is published by the American Heart Association, 7272 Greenville Avenue, Dallas, TX 75231

Copyright © 2011 American Heart Association, Inc. All rights reserved.

Print ISSN: 1079-5642. Online ISSN: 1524-4636

The online version of this article, along with updated information and services, is located on the World Wide Web at:

<http://atvb.ahajournals.org/content/31/12/e116>

Permissions: Requests for permissions to reproduce figures, tables, or portions of articles originally published in *Arteriosclerosis, Thrombosis, and Vascular Biology* can be obtained via RightsLink, a service of the Copyright Clearance Center, not the Editorial Office. Once the online version of the published article for which permission is being requested is located, click Request Permissions in the middle column of the Web page under Services. Further information about this process is available in the [Permissions and Rights Question and Answer](#) document.

Reprints: Information about reprints can be found online at:

<http://www.lww.com/reprints>

Subscriptions: Information about subscribing to *Arteriosclerosis, Thrombosis, and Vascular Biology* is online at:

<http://atvb.ahajournals.org/subscriptions/>

Heparan Sulfate Proteoglycans Mediate the Angiogenic Activity of the Vascular Endothelial Growth Factor Receptor-2 Agonist Gremlin

Paola Chiodelli, Stefania Mitola, Cosetta Ravelli, Pasqua Oreste, Marco Rusnati, Marco Presta

Objective—Heparan sulfate proteoglycans (HSPGs) modulate the interaction of proangiogenic heparin-binding vascular endothelial growth factors (VEGFs) with signaling VEGF receptor-2 (VEGFR2) and neuropilin coreceptors in endothelial cells (ECs). The bone morphogenic protein antagonist gremlin is a proangiogenic ligand of VEGFR2, distinct from canonical VEGFs. Here we investigated the role of HSPGs in VEGFR2 interaction, signaling, and proangiogenic capacity of gremlin in ECs.

Methods and Results—Surface plasmon resonance demonstrated that gremlin binds heparin and heparan sulfate, but not other glycosaminoglycans, via *N*-, 2-*O*-, and 6-*O*-sulfated groups of the polysaccharide. Accordingly, gremlin binds HSPGs of the EC surface and extracellular matrix. Gremlin/HSPG interaction is prevented by free heparin and heparan sulfate digestion or undersulfation following EC treatment with heparinase II or sodium chlorate. However, at variance with canonical heparin-binding VEGFs, gremlin does not interact with neuropilin-1 coreceptor. On the other hand, HSPGs mediate VEGFR2 engagement and autophosphorylation, extracellular signaling-regulated kinase_{1/2} and p38 mitogen-activated protein kinase activation, and consequent proangiogenic responses of ECs to gremlin. On this basis, we evaluated the gremlin-antagonist activity of a panel of chemically sulfated derivatives of the *Escherichia coli* K5 polysaccharide. The results demonstrate that the highly *N,O*-sulfated derivative K5-N,OS(H) binds gremlin with high potency, thus inhibiting VEGFR2 interaction and angiogenic activity in vitro and in vivo.

Conclusion—HSPGs act as functional gremlin coreceptors in ECs, affecting its productive interaction with VEGFR2 and angiogenic activity. This has allowed the identification of the biotechnological K5-N,OS(H) as a novel angiostatic gremlin antagonist. (*Arterioscler Thromb Vasc Biol.* 2011;31:e116-e127.)

Key Words: angiogenesis ■ endothelium ■ gremlin ■ heparan sulfate proteoglycans

Angiogenesis plays a key role in various physiological and pathological conditions, including embryonic development, wound repair, inflammation, and tumor growth.¹ Numerous inducers of angiogenesis have been identified, including the members of the vascular endothelial growth factor (VEGF) family.² Different isoforms of mammalian VEGFs interact with tyrosine kinase VEGF receptors (VEGFRs) expressed on the surface of endothelial cells (ECs)³ and with heparan sulfate (HS) proteoglycan (HSPG) and neuropilin (NRP) coreceptors,^{4,5} thus activating a proangiogenic response.

HSPGs consist of a core protein and of glycosaminoglycan (GAG) chains represented by unbranched heparin-like polysaccharides. They are found in free forms, in the extracellular matrix (ECM), or associated with the plasma membrane where they regulate the function of a wide range of ligands.^{6,7} In particular, endothelial HSPGs modulate angiogenesis by affecting bioavailability and interaction of heparin-binding VEGFs with signaling VEGFRs and NRP coreceptors.^{8,9}

Heparin/HS interaction with angiogenic growth factors depends on the degree/distribution of sulfate groups and length of the GAG chain, distinct oligosaccharide sequences mediating its binding activity.^{10–12} Moreover, the study of the biochemical bases of this interaction has been exploited to design angiostatic heparin-like compounds, chemically modified heparins, and biotechnological heparins.^{13–16}

Gremlin belongs to the CAN (Cerberus and Dan) family of cystine-knot–secreted proteins.^{17,18} It binds various bone morphogenic proteins (BMPs), thus preventing their interaction with cell surface receptors.¹⁹ The capacity of gremlin to bind BMPs and to inhibit their interaction with the cognate transforming growth factor- β (TGF- β) family receptors is thought to play a role in embryonic development of various organ systems, such as bone, kidney, and lung.^{20–22} Also, gremlin has been implicated in the pathogenesis of human diseases, including pulmonary hypertension and idiopathic pulmonary fibrosis²³ and diabetic nephropathy.²⁴ Moreover,

Received on: April 15, 2011; final version accepted on: August 30, 2011.

From the Unit of General Pathology and Immunology, Department of Biomedical Sciences and Biotechnology, School of Medicine, University of Brescia, Brescia, Italy (P.C., S.M., C.R., M.R., M.P.); Glycores 2000, Milan, Italy (P.O.).

Correspondence to Marco Presta, General Pathology, Department of Biomedical Sciences and Biotechnology, Viale Europa 11, 25123 Brescia, Italy. E-mail presta@med.unibs.it

© 2011 American Heart Association, Inc.

Arterioscler Thromb Vasc Biol is available at <http://atvb.ahajournals.org>

DOI: 10.1161/ATVBAHA.111.235184

gremlin is produced by human tumors^{25,26} and is expressed by proangiogenic ECs in vitro and tumor endothelium in vivo.²⁷ Gremlin stimulates EC intracellular signaling and migration in vitro, leading to a potent angiogenic response in vivo.^{27,28} This is due to its capacity to bind and activate VEGFR2, the main transducer of VEGF-mediated angiogenic signals, in a BMP-independent manner.²⁹ Thus, gremlin acts as a VEGFR2 agonist distinct from VEGF family members that may play paracrine/autocrine functions in tumor neovascularization.

Scattered experimental evidence indicates that gremlin may act as a heparin-binding angiogenic factor: gremlin binds to heparin-Sepharose beads²⁷; it associates to the surface of producing cells³⁰; and a heparin-binding domain has been identified in sclerostin, a BMP antagonist structurally related with gremlin.^{31,32} Here, we investigated the capacity of gremlin to interact with heparin and cell-associated HSPGs and the role of endothelial HSPGs in mediating gremlin-dependent VEGFR2 activation and angiogenic activity. The results demonstrate that gremlin binds heparin/HS. However, at variance with canonical heparin-binding VEGFR2 ligands, gremlin interacts with HSPGs but not with NRP-1 in ECs. Nevertheless, cell surface HSPGs play a nonredundant role in mediating the ability of gremlin to bind and activate VEGFR2 in endothelium, thus triggering an NRP-1-independent proangiogenic response. Accordingly, we have identified a chemically modified, heparin-like derivative of the capsular *Escherichia coli* K5 polysaccharide¹⁶ as a potent angiostatic gremlin antagonist.

Methods

Chemicals

Recombinant gremlin, anti-gremlin antibody, and human recombinant VEGF-A165 were from R&D Systems (Minneapolis, MN); anti-phospho (P)-VEGFR2 antibody was from Cell Signaling Technology (Boston, MA); anti-tubulin antibody, heparinase II, phorbol myristate acetate (PMA), and protease inhibitors were from Sigma-Aldrich (St Louis, MO); anti-P-extracellular signaling-regulated kinase (anti-P-ERK_{1/2}), anti-VEGFR2, anti-ERK₂, anti-p38, and anti-P-p38 mitogen-activated protein kinase antibodies were from Santa Cruz Biotechnology (Santa Cruz, CA); anti-actin antibody was from Chemicon, Millipore (Billerica, MA); anti-focal adhesion kinase (clone 2A7) was from Upstate, Millipore; sodium chlorate was from BDH Laboratory Supplies (Pole, United Kingdom); type I HS was from Opocrin (Corlo, Italy); and unmodified, fractionated very-low-molecular weight (MW) heparins, chemically modified heparins, and K5 polysaccharide derivatives were from Glycores 2000 (Milan, Italy). K5 derivatives were obtained by *N*-deacetylation/*N*-sulfation, *O*-sulfation, or both of a single batch of *E. coli* K5 polysaccharide (see Leali et al³³ for a description of these compounds). Dermatan sulfate, chondroitin-4-sulfate, chondroitin-6-sulfate, and hyaluronic acid were obtained from Dr M. Del Rosso, University of Florence, Italy (see Rusnati et al³⁴ for a description of these GAGs). Tinzaparin sodium was from LEO Pharmaceutical Products, Ltd (Ballerup, Denmark). The HS-specific monoclonal antibody 10E4³⁵ was kindly provided by G. David (Leuven University, Leuven, Belgium).

Surface Plasmon Resonance Analysis

Surface plasmon resonance (SPR) measurements were performed on a BIAcore X instrument (GE Healthcare). For the study of gremlin/heparin interaction, heparin was immobilized onto a CM3 sensor chip (GE Healthcare) as described.³⁶ A streptavidin-coated sensor chip was used as reference and for blank subtraction. Increasing

concentrations of gremlin in 10 mmol/L HEPES buffer (HBS-EP), pH 7.4, containing 150 mmol/L NaCl, 3 mmol/L EDTA, and 0.005% surfactant P20 (HBS-EP) (GE Healthcare) were injected over the heparin-coated or streptavidin surfaces for 4 minutes and then washed until dissociation was observed. After each run, the sensor chip was regenerated by injection of HBS-EP containing 2.0 mol/L NaCl.

In all experiments, association and dissociation rates (k_{on} and k_{off} , respectively) were obtained by fitting the raw sensorgrams with the 1:1 Langmuir binding model using the Biaevaluation software (BIAcore). Equilibrium affinity constants (expressed as dissociation constant, K_d) were either derived from the kinetic parameters ($K_d = k_{off}/k_{on}$) or determined from Scatchard plot analysis of the equilibrium binding data.

Cell Cultures

Human umbilical vein endothelial (HUVE) cells were used at early passages (passages I–IV) and grown on plastic surface coated with porcine gelatin (Sigma-Aldrich) in M199 medium (Invitrogen, Carlsbad, CA) supplemented with 20% fetal calf serum (FCS) (Invitrogen), EC growth factor (100 μ g/mL) (Sigma-Aldrich), and porcine heparin (100 μ g/mL, Sigma-Aldrich). Fetal bovine aortic endothelial GM 7373 cells³⁷ were grown in Dulbecco's modified Eagle medium (Invitrogen) containing 10% FCS, vitamins, and essential and nonessential amino acids. These cells were transfected according to standard protocols with a pcDNA3.1 expression vector harboring the mouse VEGFR2 cDNA (provided by G. Breier, Max Planck Institute, Bad Nauheim, Germany) to generate stable GM7373-VEGFR2 transfectants. Wild-type Chinese hamster ovary cells (CHO)-K1 cells and GAG-deficient A745 CHO cells³⁸ were kindly provided by J.D. Esko (University of California, La Jolla, CA) and grown in Ham's F-12 medium supplemented with 10% FCS.

To inhibit the sulfation of cell-associated HS chains, GM7373 and HUVE cells were grown for 48 hours in presence of sodium chlorate (50 and 30 mmol/L, respectively).³⁹ Alternatively, cells were incubated for 2 hours at 37°C with heparinase II (15 mU/mL in phosphate-buffered saline [PBS], Sigma-Aldrich) before experimentation.

Human pancreatic carcinoma (PANC-1) cells were grown in Dulbecco's modified Eagle medium containing 10% FCS, vitamins, and essential and nonessential amino acids. Gremlin-overexpressing PANC-1 cells (PANC-1-gremlin cells) were generated by infection with the *pRRlsin.cPPT.PGK* lentiviral vector (kindly provided by L. Naldini, San Raffaele Institute, Milan, Italy) harboring the rat gremlin cDNA.⁴⁰ Green fluorescent protein (GFP)-overexpressing PANC-1 cells (PANC-1-GFP cells) were generated with the same procedures and used as a negative control. PANC-1-GFP and PANC-1-gremlin cells were grown for 48 hours in serum-free Dulbecco's modified Eagle medium and their conditioned media were analyzed for gremlin content by Western blotting and for the capacity to induce VEGFR2 phosphorylation in HUVE cells.

Gremlin/Cell-Associated HSPG Binding Assays

CHO-K1 cells; GAG-deficient A745 CHO-K1 cells; and untreated, chlorate-treated, or heparinase II-treated GM7373 cells were incubated with gremlin (100 ng/mL) for 2 hours at 4°C in serum-free medium in the absence or in the presence of the indicated competitor. Then, cells were washed twice with PBS or with PBS plus 1.5 mol/L NaCl to remove gremlin bound to HSPGs.⁴¹ Next, immunofluorescence analysis was performed using an anti-gremlin antibody followed by Alexa Fluor 488 anti-goat IgG (Invitrogen), and cells were photographed using a Zeiss Axiovert 200M epifluorescence microscope equipped with a Plan-Apochromat $\times 63/1.4$ NA oil objective. Alternatively, HSPG-bound gremlin was collected in SDS-PAGE sample buffer and analyzed with anti-gremlin antibody by Western blotting.

In a parallel set of experiments, cell-free subendothelial ECM preparations were obtained by incubating GM7373 cells for 3 minutes at room temperature with 0.5% Triton X plus 0.00375% NH₃ in PBS.⁴² Next, cell-free ECM preparations were incubated

with gremlin and analyzed for HSPG-bound gremlin as described above.

VEGFR2 Cross-Linking Assay

Confluent GM7373-VEGFR2 cells were incubated for 2 hours at 4°C with gremlin dissolved in PBS containing the bis(sulfosuccinamide) suberate cross-linking reagent (BS3, Pierce). Then, cells were lysed in 50 mmol/L Tris-HCl buffer (pH 7.4) containing 150 mmol/L NaCl, 1% Triton X-100, 1.0 mmol/L Na₂VO₄, and protease inhibitors. Lysates were immunoprecipitated and separated by SDS-PAGE followed by Western blotting with anti-gremlin or anti-VEGFR2 antibodies.

ELISA

Ninety-six-well plates were coated for 16 hours at room temperature with the extracellular domain of soluble VEGFR2_{D1-7} (soluble VEGFR2, Calbiochem) or rat NRP-1 receptor (R&D Systems) in PBS followed by a 3-hour blocking step with 1% bovine serum albumin. Next, gremlin or VEGF-A165 (in PBS containing 0.1% bovine serum albumin, 5 mmol/L EDTA, 0.004% Tween 20 [PBET]) were sequentially incubated for 1 hour at 37°C and for 1 hour at room temperature. For competitive ELISA, gremlin was added in presence of K5 derivatives. Then, wells were further incubated for 1 hour at 37°C and for an additional 1 hour at room temperature with an anti-gremlin antibody or anti-VEGF antibody (R&D Systems), both at 100 ng/mL in PBET. Finally, wells were incubated for 1 hour at room temperature with a secondary anti-goat or anti-mouse horseradish peroxidase-conjugated antibody (Santa Cruz Biotechnology).

VEGFR2/NRP-1 Coimmunoprecipitation Analysis

Confluent HUVE cells were made quiescent by a 16-hour starvation in M199 medium containing 5% FCS. Cells were then stimulated with gremlin (50 ng/mL) or VEGF-A165 (30 ng/mL) and lysed in 50 mmol/L Tris-HCl buffer, pH 7.4, containing 150 mmol/L NaCl, 1% Triton X-100, 10% glycerol, and a protease/phosphatase inhibitors mix (Sigma-Aldrich). After centrifugation (15 minutes, 10 000g), supernatants were precleared by 1 hour of incubation with protein A-Sepharose (Sigma-Aldrich). Samples (1 mg of proteins) were incubated overnight at 4°C with rabbit polyclonal anti-VEGFR2 antibody (Santa Cruz Biotechnology), and immune complexes were recovered on protein A-Sepharose. Immunoprecipitates were washed 4 times with lysis buffer, twice with the same buffer without Triton X-100 and once with TBS. Proteins were solubilized under reducing conditions, separated by SDS-PAGE (8%), and analyzed by Western blotting with anti-NRP-1 and anti-P-VEGFR2 (Tyr1175) antibodies. Uniform immunoprecipitation was confirmed using an anti-VEGFR2 antibody.

Immunofluorescence Analysis

Cells were seeded on glass coverslips in M199 medium containing 2% FCS. Cells were treated with gremlin (100 ng/mL) for 10 minutes at 37°C, fixed in 3% paraformaldehyde/2% sucrose in PBS, permeabilized with 0.5% Triton X-100, and saturated with goat serum in PBS. Then, cells were incubated with an anti-P-VEGFR2 antibody followed by Alexa Fluor 488 anti-rabbit IgG (Invitrogen). Cells were analyzed using a Zeiss Axiovert 200M epifluorescence microscope or a LSM510 Meta confocal microscope equipped with a Plan-Apochromat ×63/1.4 NA oil objective.

Western Blot Analysis

Confluent HUVE cells were made quiescent by a 16 hours-starvation in M199 medium containing 5% FCS. After stimulation with gremlin (100 ng/mL), cells were lysed in 50 mmol/L Tris-HCl buffer, pH 7.4, containing 150 mmol/L NaCl, 1% Triton X-100, 0.1% Brij and a protease/phosphatase inhibitors mix (Sigma-Aldrich) and 50 to 100 μg aliquots of the cell extracts were analyzed by 6% to 8% SDS-PAGE followed by Western blotting with anti-P-VEGFR2, P-ERK_{1/2} or P-p38 mitogen-activated protein kinase antibodies. In

all the experiments, uniform loading of the gels was confirmed using anti-focal adhesion kinase, VEGFR2, ERK₂ or p38 antibodies.

Chemotaxis Assay

HUVE cells (1.0×10⁶ cells/mL) were seeded in M199 medium containing 2% FCS in the upper compartment of a Boyden chamber containing gelatin-coated polyvinylpyrrolidone-free polycarbonate filters (8 μm pore size, Costar, Cambridge, MA). Gremlin (10 ng/mL) or PMA (100 ng/mL) in M199 containing 2% FCS was placed in the lower compartment. A 2% FCS medium was used as negative control. After 4 hours of incubation at 37°C, cells that had migrated to the lower side of the filter were stained with Diff-Quik (Dade-Behring, Milan, Italy). Five random fields were counted for each triplicate sample.

Cell Motility Assay

Cell motility was assessed by time-lapse videomicroscopy. Cells were seeded at 150 cells/cm² in 24-well plates for 2 hours and then stimulated with gremlin (100 ng/mL). Constant temperature (37°C) and pCO₂ (5%) were maintained throughout the experimental period by means of an heatable stage and climate chamber. Cells were observed under an inverted photomicroscope (Zeiss Axiovert 200M), and phase-contrast snap photographs (1 frame every 8 minutes) were digitally recorded for 360 minutes. Cell paths (25–30 cells per experimental point) were generated from centroid positions and migration parameters were analyzed with the Chemotaxis and Migration tool of ImageJ software (<http://rsbweb.nih.gov/ij/>).

EC Sprouting Assay

Sprouting of HUVE cell aggregates embedded in fibrin gel was analyzed as described.²⁷ Briefly, spheroids were prepared in 20% methylcellulose medium, embedded in fibrin gel, and stimulated with gremlin (50 ng/mL) in the absence or in the presence of K5 derivatives. Formation of radially growing cell sprouts was observed during the next 24 hours and photographed at a ×200 magnification using an Axiovert 200M microscope equipped with a ×20 objective (LD A Plan 20×/0.30PH1, Zeiss).

Chick Embryo Chorioallantoic Membrane Assay

Alginate beads (5 μL) containing vehicle or gremlin (100 ng/bead) were placed on the chorioallantoic membrane of fertilized white Leghorn chicken eggs at day 11 of incubation²⁸ in the absence or in the presence of K5 or K5-N,OS(H) (both at 1 μg/bead). After 72 hours, newly formed blood vessels converging toward the implant were counted at a ×5 magnification using a STEMI SR stereomicroscope equipped with an objective *f* of 100 mm with adapter ring 475070 (Zeiss).

Human Artery Ring Assay

One-millimeter human umbilical artery rings were embedded in fibrin gel²⁸ in the presence of the conditioned medium from PANC-1-GFP or PANC-1-gremlin cells in the absence or in the presence of 100 ng/mL K5 derivatives. After 6 days, EC sprouts, morphologically distinguishable from scattering fibroblasts/smooth muscle cells, were counted. Then, rings were photographed at a ×100 magnification using an Axiovert 200M microscope equipped with a ×20 objective (LD A PLAN 20X/0.30PH1, Zeiss).

Statistical Analysis

Data were expressed as mean±SD. The analysis was performed using ANOVA models with probability values correction for multiple comparisons.⁴³

Results

Characterization of Gremlin/Heparin Interaction

Real-time SPR analysis was exploited to characterize gremlin/heparin interaction. Increasing concentrations of gremlin were injected over a streptavidin-activated BIAcore sensor

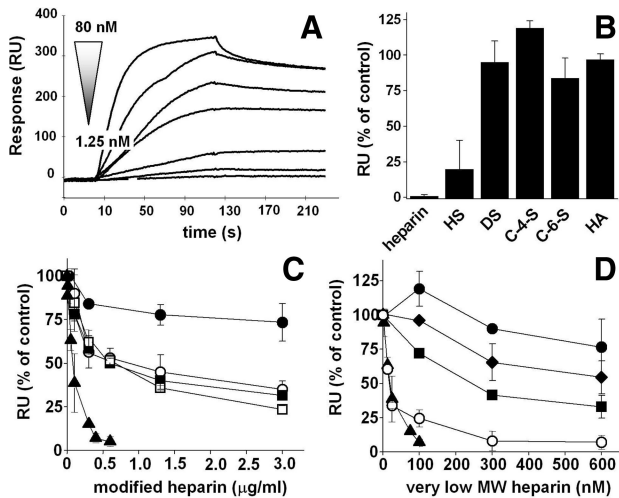


Figure 1. Surface plasmon resonance (SPR) analysis of gremlin/heparin interaction. **A**, Sensorgram overlay showing the binding of increasing amounts of gremlin (1.25, 2.5, 5.0, 10.0, 20.0, 40.0, and 80.0 nmol/L) to a heparin-coated BIACore sensor chip. The response (in resonance units [RU]) was recorded as a function of time. **B** to **D**, SPR competitive studies performed by injecting gremlin (20 nmol/L) on the heparin surface in the presence of different glycosaminoglycans (all at 1.0 $\mu\text{g/ml}$) (**B**); increasing concentrations of unmodified heparin (\blacktriangle), *N*-desulfated/*N*-acetylated heparin (\circ), 6-*O*-desulfated heparin (\blacksquare), 2-*O*-desulfated heparin (\square), and totally *O*-desulfated heparin (\bullet) (**C**); or increasing concentrations of unmodified heparin (\blacktriangle), very-low-molecular weight (MW) 4.0-kDa heparin (\blacksquare), 3.0-kDa heparin (\blacklozenge), 2.1-kDa heparin (\bullet), or tinzaparin (\circ) (**D**). The response (in RU) was recorded at the end of the injection. Each point is the mean \pm SD of 2 or 3 independent experiments. HS indicates heparan sulfate; DS, dermatan sulfate; C-4-S, chondroitin-4-sulfate; C-6-S, chondroitin-6-sulfate; HA, hyaluronic acid.

chip coated with biotinylated heparin (Figure 1A). Analysis of kinetic parameters (k_{on} and $k_{\text{off}} = 1.86 \times 10^5 \text{ [mol/L]}^{-1} \text{ per second}^{-1}$ and $3.66 \times 10^{-3} \text{ per second}^{-1}$, respectively), and Scatchard plot analysis of steady-state SPR (data not shown) demonstrates that gremlin/heparin interaction occurs with high affinity ($K_d = 20 \text{ nmol/L}$).

The capacity of different GAGs to inhibit the binding of gremlin to immobilized heparin was then evaluated in a SPR competition assay (Figure 1B). Free heparin and HS prevented the binding of gremlin to immobilized heparin with ID_{50} values of 0.12 and 0.7 $\mu\text{g/ml}$, respectively (data not shown), whereas dermatan sulfate, chondroitin-4-sulfate, chondroitin-6-sulfate, and hyaluronic acid were ineffective. Thus, GAG/gremlin interaction depends, at least in part, on differences in GAG structure and degree of sulfation. On this basis, selectively desulfated heparins were evaluated in the SPR competition assay (Figure 1C). No competition was exerted by totally *O*-desulfated heparin, whereas 2-*O*-desulfated, 6-*O*-desulfated, and *N*-desulfated/*N*-acetylated heparins show a significant reduction in the capacity to inhibit the binding of gremlin to the heparin-coated sensor chip ($\text{ID}_{50} = 0.6, 0.6, \text{ and } 0.9 \mu\text{g/ml}$, respectively) compared with unmodified heparin ($\text{ID}_{50} = 0.12 \mu\text{g/ml}$). Taken together, the data indicate that at least some 2-*O*-, 6-*O*-, and *N*-sulfate groups must be organized on the same heparin chain to allow an optimal interaction with gremlin.

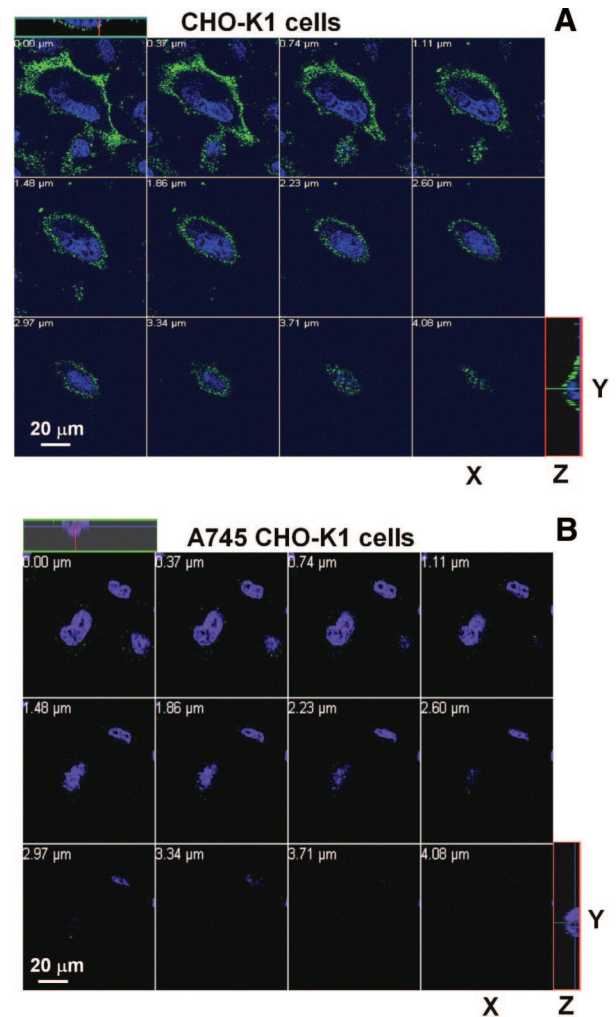


Figure 2. Confocal analysis of gremlin binding to cell-surface heparan sulfate proteoglycans (HSPGs). CHO-K1 cells (**A**) and glycosaminoglycan-deficient A745 CHO-K1 cells (**B**) were incubated with gremlin (100 ng/ml) for 2 hours at 4°C. At the end of incubation, nonpermeabilized cells were decorated with anti-gremlin antibody (in green) and 4',6-diamidino-2-phenylindole (in blue). z-Stack sections and orthogonal z reconstitution were analyzed by confocal microscopy.

Also, the influence of the length of the heparin chain on its binding activity was investigated by using tinzaparin, a therapeutic low-MW heparin whose MW ranges between 5.5 and 7.5 kDa,⁴⁴ and 3 different very-low-MW heparins (average MWs of 4.0, 3.0, and 2.1 kDa, respectively). On a molar basis, tinzaparin binds gremlin with an affinity that is similar to unmodified heparin, whereas the capacity of very-low-MW heparins to bind gremlin is progressively reduced as a function of size, with 2.1-kDa heparin showing the weakest activity (Figure 1D).

Gremlin Binds EC-Associated HSPGs

We then evaluated the capacity of gremlin to interact with cell-associated HSPGs. In a first set of experiments, HSPG-bearing CHO-K1 cells and GAG-deficient A745 CHO-K1 cell mutants⁴⁵ were incubated with gremlin at 4°C to prevent the internalization of the protein and decorated with anti-gremlin antibody. Confocal microscopy (Figure 2) and immunofluorescence analysis (Figure 3A) demonstrated the capacity of gremlin

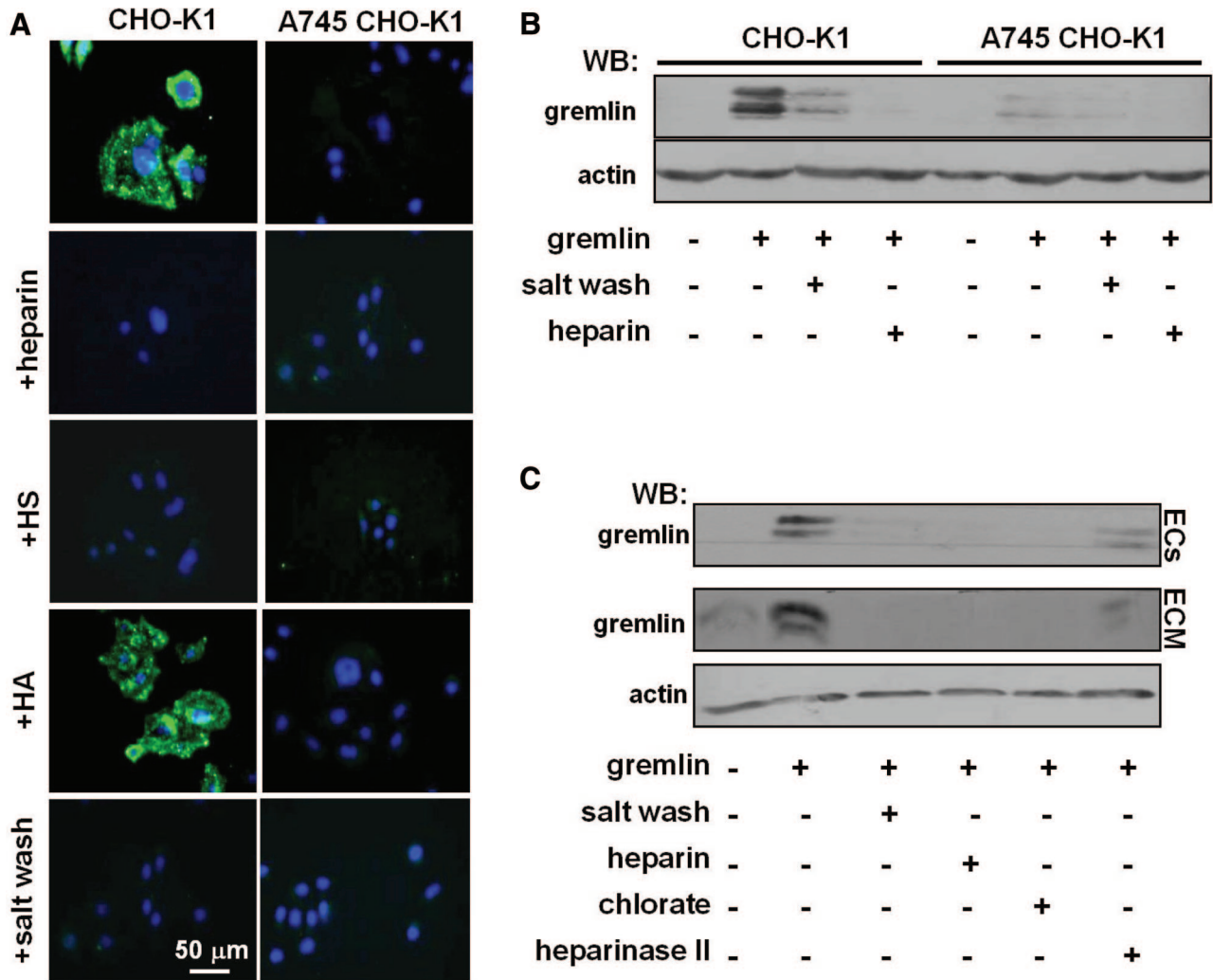


Figure 3. Binding of gremlin to cell-associated heparan sulfate proteoglycans (HSPGs). **A**, CHO-K1 cells and glycosaminoglycan-deficient A745 CHO-K1 cell mutants were incubated for 2 hours at 4°C with gremlin alone (100 ng/mL) or in the presence of heparin, heparan sulfate (HS), or hyaluronic acid (HA) (all at 1.0 μ g/mL). Then, nonpermeabilized cells were washed with PBS or with PBS plus 1.5 mol/L NaCl (salt wash) and decorated with an anti-gremlin antibody (in green) followed by nuclear counterstaining with 4',6-diamidino-2-phenylindole (in blue). **B**, CHO-K1 and A745 CHO-K1 cells were incubated with gremlin as in **A**, and cell lysates were analyzed by Western blot (WB) with an anti-gremlin antibody. **C**, Subendothelial extracellular matrices (ECMs) were prepared from untreated or chlorate- or heparinase II-treated GM7373 cell monolayers. Then, living cells or their ECMs were incubated for 2 hours at 4°C with gremlin (100 ng/mL) in the absence or in the presence of heparin (1.0 μ g/mL), washed with PBS or with PBS plus 1.5 mol/L NaCl (salt wash) and analyzed by Western blotting with an anti-gremlin antibody. Uniform loading of the samples was confirmed by Western blotting with an anti-actin antibody. The data are representative of 2 or 3 independent experiments that gave similar results.

to bind the surface of CHO-K1 cells but not of GAG-deficient A745 CHO-K1 cells. The binding of gremlin to CHO-K1 cell surface was inhibited by free heparin or HS, whereas hyaluronic acid was ineffective. Also, in keeping with a postulated HSPG interaction, a 1.5 mol/L NaCl wash detached gremlin bound to the CHO-K1 cell surface. Similar results were obtained when cell-surface bound gremlin was analyzed by Western blotting of the cell monolayers (Figure 3B).

We then evaluated the capacity of gremlin to bind EC-associated HSPGs. In keeping with the data obtained with CHO-K1 cells, immunofluorescence analysis revealed that gremlin binds the surface of bovine aortic endothelial GM7373 cells and that the binding is competed by heparin or abrogated by a 1.5 mol/L NaCl wash (data not shown). Accordingly, digestion of cell-associated HSPGs by heparinase II or inhibition of the sulfation of the HS chains by

pretreatment of ECs with sodium chlorate both prevented the binding of gremlin to the EC surface (Figure 3C). Similar results were obtained with HUVE cells (see below).

Finally, we analyzed the capacity of gremlin to bind HSPGs associated with the cell-free subendothelial ECM deposited by GM7373 cells (Figure 3C). Also in this case, binding of gremlin to subendothelial ECM was prevented by digestion with heparinase II, pretreatment of ECs with chlorate before ECM isolation, or coincubation with heparin. Again, a 1.5 mol/L NaCl wash was able to remove gremlin from subendothelial ECM-associated HSPGs.

HSPGs Are Required for VEGFR2 Binding and Activation by Gremlin

Previous observations had implicated HSPGs in the interaction of heparin-binding VEGF isoforms with tyrosine kinase-

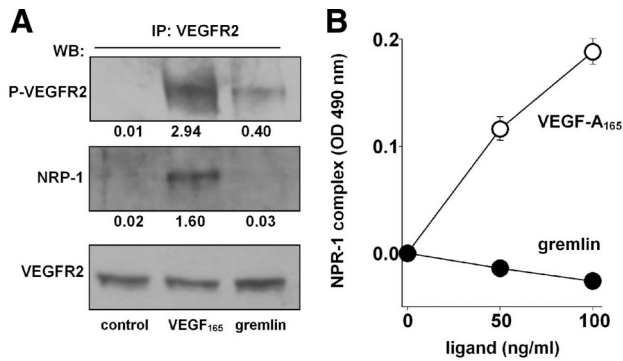


Figure 4. Gremlin does not interact with neuropilin-1 (NRP-1). **A**, Quiescent human umbilical vein endothelial (HUVE) cells were incubated for 15 minutes at room temperature in the absence (control) or in the presence of vascular endothelial growth factor (VEGF)-A₁₆₅ (30 ng/mL) or gremlin (50 ng/mL), lysed, and immunoprecipitated (IP) with anti-VEGF receptor-2 (VEGFR2) antibody, and immunocomplexes were probed in a Western blot (WB) with anti-P-VEGFR2 or anti-NRP-1 antibodies. Uniform loading of the gel was confirmed by WB with anti-VEGFR2 antibody. The P-VEGFR2/VEGFR2 and NRP-1/VEGFR2 ratios are shown at the bottom of the corresponding blots, as calculated by densitometric measurement of the bands. **B**, 96-well plates coated with 2 μ g/mL NRP-1 were incubated with increasing concentrations of VEGF-A₁₆₅ or gremlin. Then, the capacity of VEGF-A₁₆₅ or gremlin to bind to the immobilized receptor was assessed by incubation with anti-VEGF-Ala or anti-gremlin antibodies, respectively.

VEGFR2 and NRP-1 coreceptor in ECs.^{4,46} However, at variance with the prototypic heparin-binding VEGFR2 ligand VEGF-A₁₆₅ and similar to VEGF-A₁₂₁ that lacks the heparin/NRP-1 binding domain,^{4,47} gremlin does not induce VEGFR2/NRP-1 complex formation when administered to HUVE cells (Figure 4A), thus indicating that HSPG interaction is not per se sufficient to drive NRP-1 engagement. Also, gremlin does not directly bind recombinant NRP-1 produced in mammalian cells in ELISA (Figure 4B) or NRP-1 expressed on HUVE cells in cross-linking experiments (data not shown). Thus, gremlin appears to differ from canonical heparin-binding VEGFs in the ability to co-opt VEGFR2 coreceptors.

On this basis, we investigated whether HSPG coreceptors play any role in mediating a productive interaction of gremlin with VEGFR2.²⁹ In a first set of experiments, we exploited VEGFR2-overexpressing endothelial GM7373 cells (GM7373-VEGFR2 cells) that express HSPGs and high levels of VEGFR2 on their cell surface (Figure 5). These cells were incubated at 4°C with gremlin in the presence of the bis(sulfosuccinamide)suberate cross-linking reagent BS3. After incubation, cell lysates were immunoprecipitated with anti-gremlin antibodies, and immunocomplexes were analyzed by Western blotting with anti-VEGFR2 antibodies. When cross-linked to the GM7373-VEGFR2 cell surface, gremlin forms a 250-kDa VEGFR2 complex whose formation is abrogated when the cross-linking reaction was performed in chlorate-treated cells (Figure 6A). Accordingly, chlorate pretreatment abolished the capacity of gremlin to induce VEGFR2 autophosphorylation in HUVE cells, as shown by immunostaining of intact cells and Western blotting of the cell extracts using an anti-P-VEGFR2 antibody

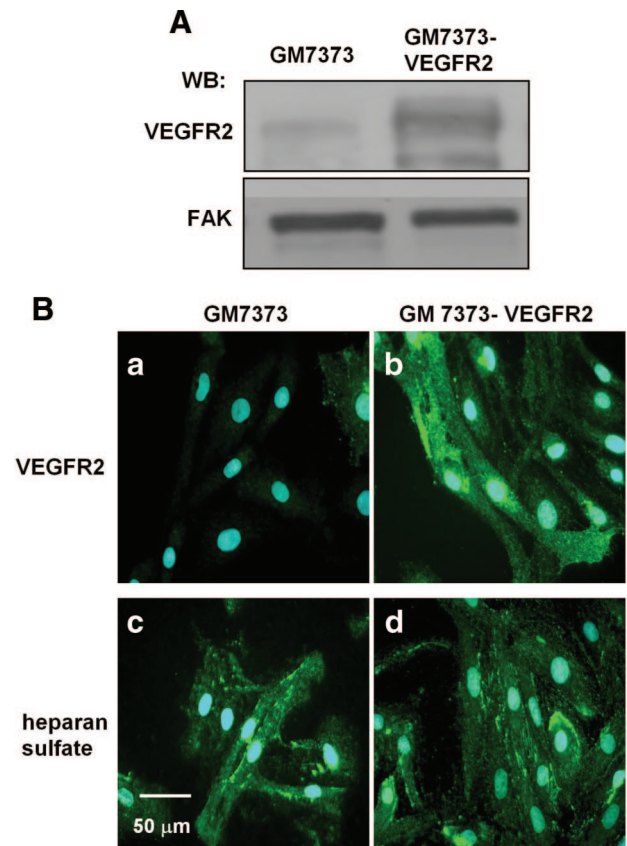


Figure 5. Heparan sulfate proteoglycan (HSPG) and vascular endothelial growth factor receptor-2 (VEGFR2) expression by endothelial GM7373-VEGFR2 cells. Parental and VEGFR2-overexpressing endothelial GM7373 cells were analyzed for VEGFR2 expression by Western blotting (WB) of the cell lysates (**A**) and by immunofluorescence analysis with an anti-VEGFR2 antibody (**B**, a and b). Cells were also decorated with the anti-heparan sulfate monoclonal antibody 10E4 (**B**, c and d). In **B**, cells were also counterstained with 4',6-diamidino-2-phenylindole (in cyan).

(Figure 6B and 6C). Also, the capacity of gremlin to induce ERK_{1/2} and p38 mitogen-activated protein kinase phosphorylation was hampered in chlorate-pretreated HUVE cells (Figure 6C). Similar results were obtained when HUVE cells were incubated with heparinase II before gremlin stimulation (data not shown). Also, addition of increasing concentrations of unmodified heparin to the cell culture medium restored the capacity of gremlin to induce VEGFR2 autophosphorylation in chlorate-pretreated HUVE cells (Figure 6D). It must be pointed out that even though chlorate pretreatment prevented the binding of gremlin to the HUVE cell surface (Figure 7A), it did not affect cell viability and the capacity of the protein kinase C activator PMA to induce ERK_{1/2} phosphorylation in these cells (Figure 7B and 7C), confirming the specificity of the effect. Taken together, these observations demonstrate that HSPGs are required for a productive interaction of gremlin with VEGFR2.

HSPGs Mediate the Angiogenic Activity of Gremlin

Stimulation of EC motility is part of the VEGFR2-dependent angiogenic program activated by gremlin.^{27,29} To assess the

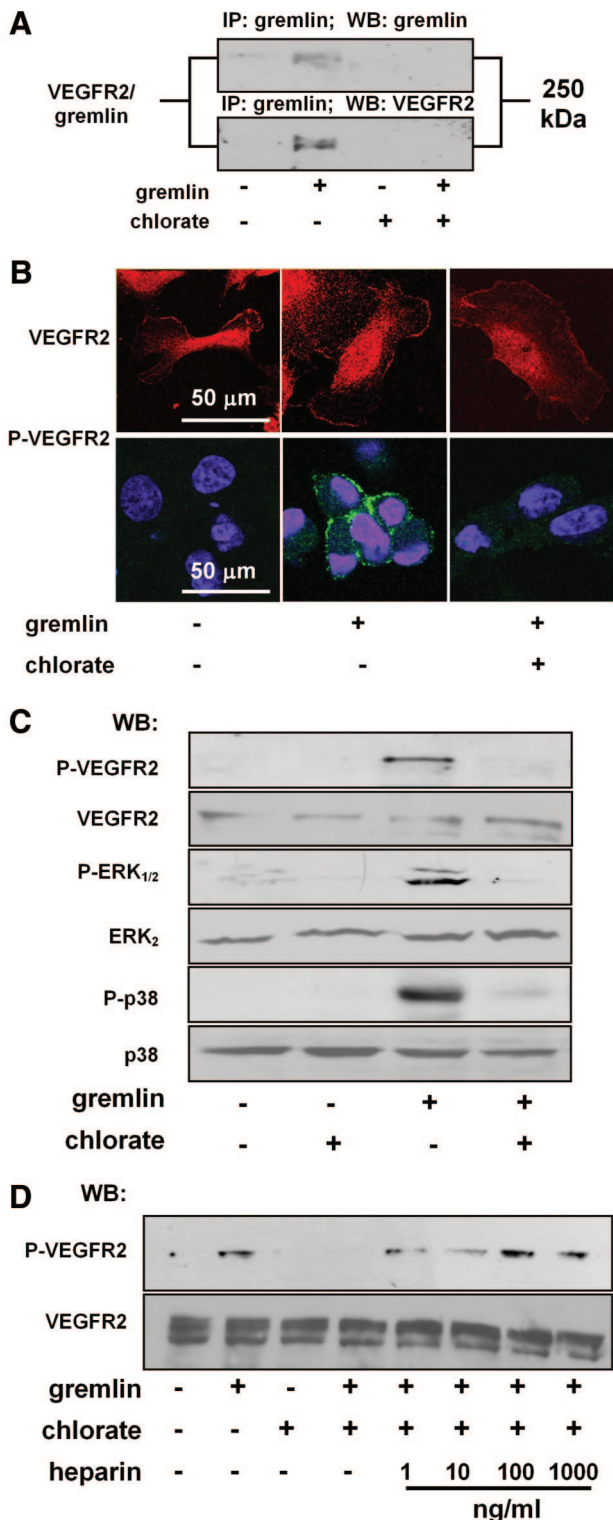


Figure 6. Endothelial heparan sulfate proteoglycans (HSPGs) mediate vascular endothelial growth factor receptor-2 (VEGFR2)/gremlin interaction and signaling. **A**, Control and chlorate-treated GM7373-VEGFR2 cells were incubated for 2 hours at 4°C with gremlin (100 ng/mL). After a further incubation with the cross-linking reagent BS3, cell lysates (1.0 mg) were immunoprecipitated with anti-gremlin antibody and probed with the same antibody or with an anti-VEGFR2 antibody in a Western blot. **B**, Serum-starved control and chlorate-treated human umbilical vein endothelial (HUVE) cells were stimulated for 10 minutes at 37°C with gremlin (100 ng/mL), decorated with

role of HSPGs in mediating the angiogenic activity of gremlin, chlorate-pretreated HUVE cells were tested in a Boyden chamber assay for their capacity to migrate through a gelatin-coated filter in response to gremlin. Despite a similar capacity to adhere to immobilized gelatin (Figure 7D) and to migrate in response to PMA (Figure 8A), chlorate-pretreated HUVE cells displayed a dramatic reduction in their chemotactic response to gremlin compared with control cells (Figure 8A). Again, HSPG digestion following heparinase II incubation mimicked the effect of chlorate, thus abolishing the chemotactic activity of gremlin in HUVE cells (data not shown). In keeping with these observations, chlorate pretreatment abolished the motogenic response of HUVE cells to gremlin as assessed by time-lapse microscopy, without affecting EC motility induced by PMA (Figure 8B). Moreover, as observed for gremlin-induced VEGFR2 autophosphorylation (see Figure 6D), addition of heparin to chlorate-treated cells restored their motogenic response to gremlin stimulation (Figure 8C).

To confirm the role of HSPGs in mediating EC activation by gremlin, spheroids of chlorate or heparinase II-treated HUVE cells were embedded in a 3-dimensional fibrin gel and stimulated with gremlin.²⁹ As shown in Figure 8D and 8E, HSPG digestion or undersulfation caused a significant reduction in the number and length of EC sprouts induced by gremlin.

Heparin-Like K5 Derivatives as Gremlin Antagonists

The capsular *E. coli* K5 polysaccharide has the same structure as the heparin precursor *N*-acetyl heparosan.¹⁶ K5 derivatives can be generated by chemical sulfation in the *N*- or *O*-position, leading to heparin-like molecules with defined sulfation patterns⁴⁸ and able to hamper the angiogenic activity of the heparin-binding fibroblast growth factor-2.³³

To assess their ability to act as gremlin antagonists, a panel of selectively sulfated K5 derivatives (including the *N*-sulfated derivative K5-NS; the *O*-sulfated derivatives with low and high degrees of sulfation, K5-OS(L) and K5-OS(H); and the *N,O*-sulfated derivatives with low and high degrees of sulfation, K5-N,OS(L) and K5-N,OS(H))³³ were evaluated for their capacity to prevent gremlin/heparin interaction in a SPR competition assay. As shown in Figure 9A, K5-N,OS(H) and K5-N,OS(L) competed for the binding of gremlin to immobilized heparin with high potency (ID₅₀ of 0.05 and 0.2

anti-VEGFR2 or anti-P-VEGFR2 antibodies (in green) followed by nuclear counterstaining with 4',6-diamidino-2-phenylindole (in blue), and observed under a confocal microscope. **C**, Serum-starved control and chlorate-treated HUVE cells were stimulated for 10 minutes at 37°C with gremlin (100 ng/mL) and cell lysates (50 μ g) were analyzed by Western blotting with anti-P-VEGFR2, anti-P-extracellular signaling-regulated kinase (P-ERK_{1/2}) or anti-P-p38 mitogen-activated protein kinase (MAPK) antibodies (p38). **D**, Serum-starved chlorate-treated HUVE cells were incubated for 10 minutes at 37°C with gremlin (100 ng/mL) and increasing concentrations of heparin. Then, cell lysates (50 μ g) were analyzed by Western blotting with anti-P-VEGFR2 antibody. Uniform loading of the gels was confirmed by incubation of the membranes with antibodies directed against the unphosphorylated form of the antigen. The data are representative of 2 or 3 independent experiments that gave similar results.

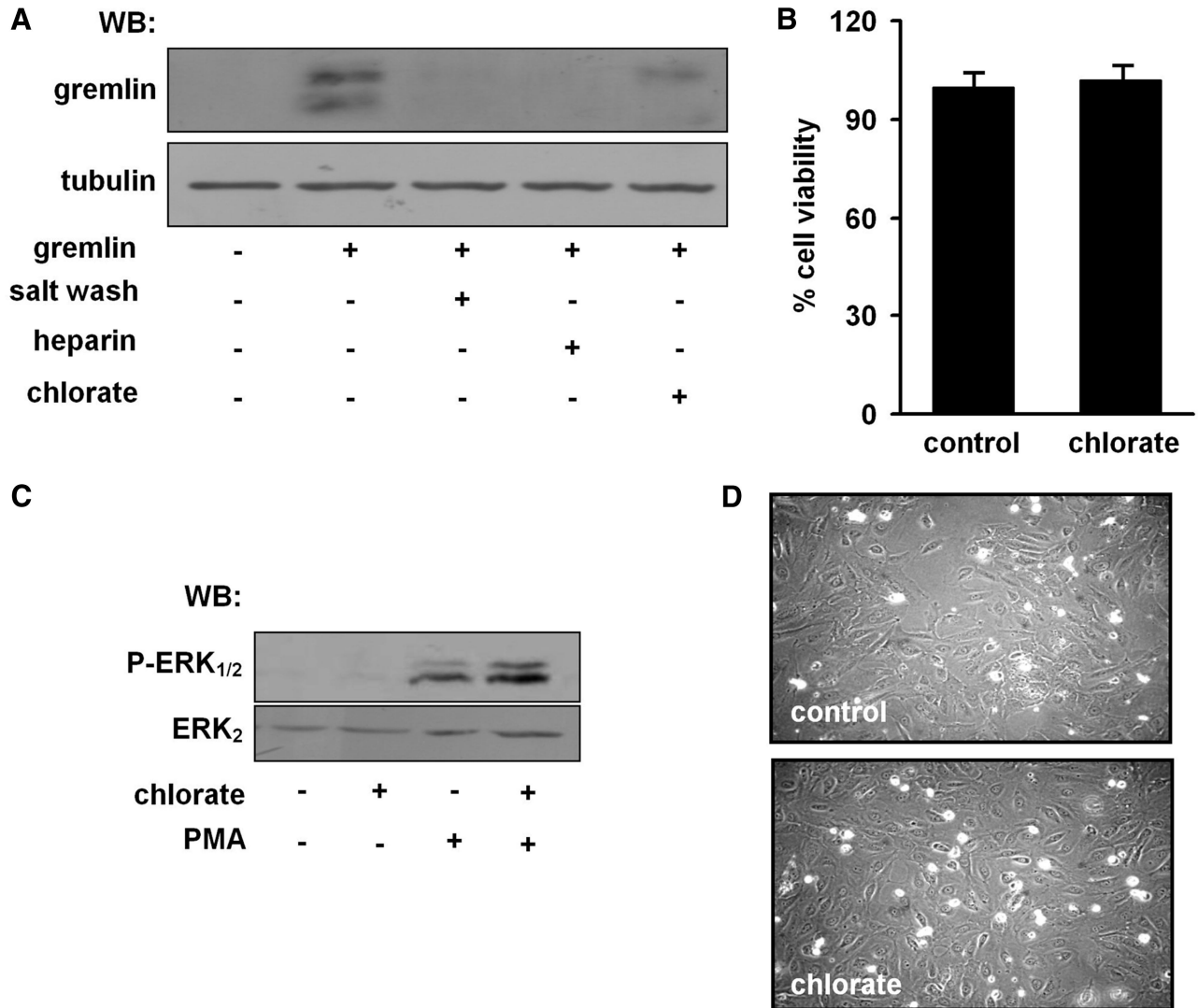


Figure 7. Characterization of chlorate-treated human umbilical vein endothelial (HUVE) cells. **A**, HUVE cell monolayers were left untreated or treated with chlorate. Then, cells were incubated for 2 hours at 4°C with gremlin (100 ng/mL) in the absence or in the presence of heparin (1 μg/mL), washed with PBS or with PBS plus 1.5 mol/L NaCl (salt wash). Then, cell lysates were analyzed by Western blotting with an anti-gremlin antibody. Uniform loading of the samples was confirmed by incubation of the membrane with an anti-tubulin antibody. **B**, Control and chlorate-treated HUVE cells were assessed for cell viability by the tetrazolium salt (3-[4,5-dimethylthiazol-2-yl]-2,5-diphenyltetrazolium bromide) colorimetric assay according to standard procedures. **C**, Control and chlorate-treated HUVE cells were stimulated for 10 minutes with phorbol myristate acetate (PMA) (10 ng/mL). Then, 50 μg-aliquots of cell lysates were analyzed by Western blotting with an anti-P-extracellular signaling-regulated kinase (P-ERK_{1/2}) antibody. Uniform loading of the gel was confirmed by incubation of the membrane with an anti-ERK₂ antibody. **D**, Control and chlorate-treated HUVE cells were allowed to adhere onto substrate-immobilized gelatin for 2 hours at room temperature, and attached cells were photographed under an inverted microscope.

μg/mL, respectively), whereas K5-OS(H) and K5-OS(L) were less effective (ID₅₀ of 0.5 and 1.0 μg/mL, respectively). K5-NS and unmodified K5 did not exert a significant competition.

Then, the most active derivative K5-N,OS(H) was tested for the capacity to affect the angiogenic activity exerted by gremlin in vitro and in vivo. As shown in Figure 9B and 9C, K5-N,OS(H) inhibits the binding of gremlin to the extracellular domain of VEGFR2 in a competitive ELISA and its ability to stimulate the sprouting of HUVE cell aggregates in fibrin gel. Also, K5-N,OS(H) exerts a potent inhibitory activity on blood vessel formation triggered by gremlin delivered on the top of the chick embryo chorioallantoic

membrane via an alginate pellet implant (Figure 9D and 9E). Accordingly, K5-N,OS(H) inhibits the angiogenic activity exerted by gremlin in a tumor-driven ex vivo angiogenesis assay in which fibrin-embedded human umbilical cord artery rings²⁸ are grown in the presence of the conditioned medium from gremlin-overexpressing human pancreatic carcinoma PANC-1 cells (Figure 10A and 10B). As shown in Figure 10C and 10D, PANC-1-gremlin cells, but not control PANC-1-GFP cells, induce a dramatic increase in the formation of EC sprouts from human artery rings that is significantly inhibited by K5-N,OS(H). When tested under the same experimental conditions, unmodified K5 was ineffective in all these assays.

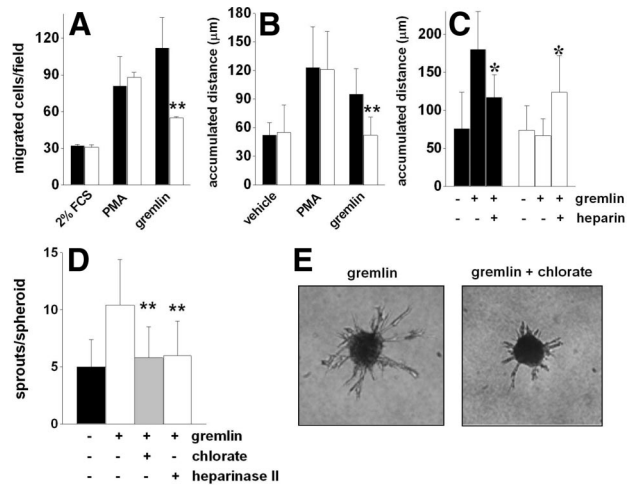


Figure 8. Heparan sulfate proteoglycans (HSPGs) mediate the angiogenic activity of gremlin in endothelial cells (ECs). **A** and **B**, Control (black bars) and chlorate-treated (open bars) human umbilical vein endothelial (HUVE) cells were assessed for their capacity to migrate in response to gremlin or phorbol myristate acetate (PMA) in a modified Boyden chamber assay (**A**) or by time-lapse videomicroscopy (**B**). **C**, Control (black bars) and chlorate-treated (open bars) HUVE cells were incubated with gremlin in the absence or in the presence of heparin (0.5 μg/mL) and assessed for their motility by time-lapse microscopy. **D**, HUVE cell spheroids obtained from control, chlorate-treated, or heparinase II-treated cells were embedded in fibrin gel and incubated with gremlin. Formation of radially growing cell sprouts was evaluated after 24 hours of incubation. **E**, Representative microphotographs of control and chlorate-treated HUVE cell spheroids stimulated with gremlin. In **A** to **D**, each data are the mean±SD of 2 or 3 independent experiments. Significantly different from gremlin alone under the same experimental conditions: **P*<0.004, ***P*<0.001. FCS, fetal calf serum.

Discussion

This is the first characterization of the interaction of gremlin with heparin/HSPGs and of its role in mediating the angiogenic response triggered by this noncanonical VEGFR2 ligand in ECs. Compared with other sulfated GAGs, heparin ($SO_3^-/COO^- = 2.14$)³⁴ binds gremlin with high affinity ($K_d = 20$ nmol/L). In HS ($SO_3^-/COO^- \cong 1.0$),³⁴ sulfate groups are arranged in high-charge-density clusters intercalated with low-charge-density regions,⁴⁹ thus resulting in a lower gremlin-binding activity. On the other hand, HS is a much more effective gremlin interactor than dermatan sulfate, chondroitin-4-sulfate, or chondroitin-6-sulfate, even though they all share a similar charge, no significant binding being observed with the nonsulfated hyaluronic acid and K5 polysaccharide. Also, similar to other heparin-binding angiogenic proteins^{10,14} the affinity for gremlin is affected by the size of the polysaccharide chain. Indeed, whereas low-MW heparin tinzaparin binds gremlin with an affinity similar to unfractionated heparin, very-low-MW heparins showed a reduced interaction, and a negligible binding was observed for 2.1-kDa heparin. Interestingly, when compared with different low-MW heparin preparations, tinzaparin has demonstrated significant antiangiogenic and anticancer properties.⁴⁴ Several sets of experimental evidence demonstrate that physicochemical and biological properties of different low-MW heparins are not alike.⁴⁴ Even though additional studies are

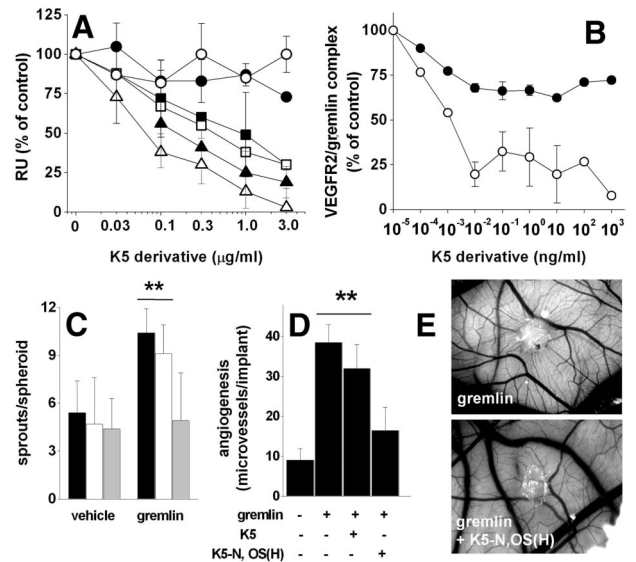


Figure 9. Sulfated K5 derivatives inhibit the angiogenic activity of gremlin. **A**, Gremlin (20 nmol/L) was injected over a heparin-coated BIAcore sensor chip in the presence of increasing concentrations of K5 (●), K5-NS (○), K5-OS(L) (■), K5-N,OS(L) (▲), K5-OS(H) (□), or K5-N,OS(H) (△), and the response (in resonance units [RU]) was recorded at the end of the injection. **B**, 96-well plates coated with the extracellular domain of soluble-vascular endothelial growth factor receptor-2 (sVEGFR2)_{D1-7} (200 ng/mL) were incubated with gremlin (50 ng/mL) in presence of increasing concentrations of K5 (●) or K5-N,OS(H) (○). Then, the formation of VEGFR2/gremlin complex was assessed by incubation with an anti-gremlin antibody. **C**, Human umbilical vein endothelial (HUVE) cell spheroids embedded in fibrin gel were incubated with vehicle or gremlin in the absence (black bars) or in the presence of K5 (open bars) or K5-N,OS(H) (gray bars) (both at 10 ng/mL). Formation of radially growing cell sprouts was evaluated after 24 hours of incubation. **D**, Alginate pellets containing gremlin (100 ng/pellet) in the absence or in the presence of K5 or K5-N,OS(H) (both at 1 μg/pellet) were implanted on chick embryo chorioallantoic membranes (10 eggs per group). After 3 days, newly formed microvessels converging vs the implant were counted. **E**, Representative images of chorioallantoic membranes implanted with alginate pellets containing gremlin alone or gremlin added with K5-N,OS(H). Note the numerous newly formed thin microvessels converging in a spoke-wheel pattern vs the gremlin implant, significantly reduced in the presence of K5-N,OS(H). Significantly different from controls: ***P*<0.001.

required to fully characterize the interaction of gremlin with different heparin preparations, our data clearly indicate that the degree of sulfation, charge distribution, disaccharide composition, and size are all important in determining the capacity of sulfated GAGs to bind gremlin.

Previous observations had shown that fibroblast growth factor-2 binds avidly to a pentasaccharide region in which *N*-sulfate groups and a single 2-*O*-sulfate group are essential for interaction. In contrast, *N*-sulfation and 6-*O*-sulfation are crucial for VEGF-A165 binding, whereas 2-*O*-sulfate groups are less essential.⁵⁰ Our data demonstrate that selective 2-*O*-, 6-*O*-, or *N*-desulfation significantly reduces gremlin/heparin interaction, indicating that they are all required for high affinity binding. These findings support the hypothesis that heparin-binding cytokines may bind sulfated GAGs in a distinct manner. Even though specific factor binding sequences may be hidden in heparin because of its high degree

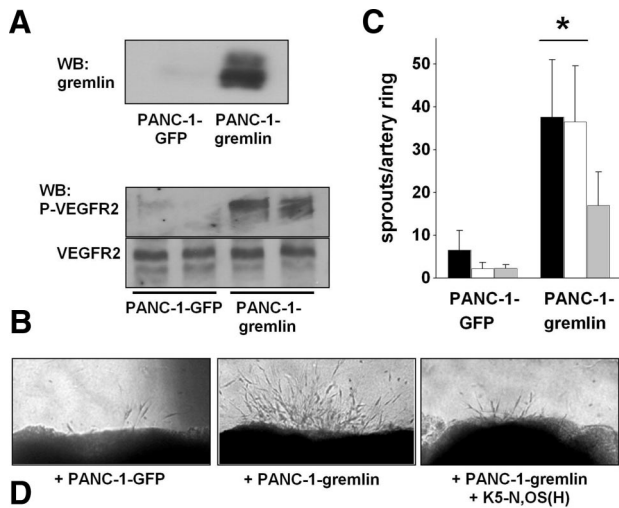


Figure 10. K5-N,OS(H) inhibits the angiogenic activity of gremlin-overexpressing human pancreatic carcinoma-1 (PANC-1) cells. **A**, Conditioned media from PANC-1-green fluorescent protein (GFP) and PANC-1-gremlin cells grown for 48 hours in serum-free Dulbecco's modified Eagle medium (DMEM) were analyzed by Western blotting with an anti-gremlin antibody. **B**, Human umbilical vein endothelial (HUVE) cells were stimulated for 15 minutes with the conditioned medium from PANC-1-GFP or PANC-1-gremlin cells. Then, 50 μ g-amounts of cell extracts were analyzed by Western blotting with an anti-P-vascular endothelial growth factor receptor-2 (VEGFR2) antibody. Uniform loading of the gel was confirmed by incubation of the membrane with an anti-VEGFR2 antibody. PANC-1-gremlin cells released gremlin in a bioactive form, as demonstrated by the capacity of their conditioned medium to induce VEGFR2 phosphorylation in HUVE cells. **C** and **D**, Human umbilical artery rings (4 rings per group) were embedded in fibrin gel and stimulated with the conditioned medium from PANC-1-GFP or PANC-1-gremlin cells in the absence (black bars) or in the presence of K5 (open bars) or K5-N,OS(H) (gray bars) (both at 100 ng/mL). After 6 days, endothelial cell (EC) sprouts were counted (**C**) and photographed under an inverted microscope at a $\times 200$ magnification (**D**). Significantly different from controls: * $P < 0.03$.

of sulfation, the high heterogeneity in HS structure allows a more refined tailoring of selective binding regions that may influence the biological activity and bioavailability of heparin/HS-binding growth factors.

In keeping with its heparin/HS binding capacity, gremlin binds the surface of CHO-K1 cells but not of GAG-deficient A745 CHO-K1 cells. Accordingly, gremlin binds HSPGs exposed on the surface of ECs and deposited in the subendothelial ECM, the binding being prevented by HS chain digestion with heparinase II or by inhibition of HS chain sulfation following EC treatment with chlorate. Similar to the canonical heparin-binding VEGFR2 ligand VEGF-A165, HSPG interaction appears to be essential for the binding of gremlin to VEGFR2 and receptor activation in ECs. Indeed, chlorate treatment or heparinase II digestion both hamper gremlin/VEGFR2 interaction in HUVE cells. Accordingly, VEGFR2 autophosphorylation triggered by gremlin is abolished following HS digestion or undersulfation, yet is restored by the addition of exogenous heparin. Similarly, inhibition of HSPG interaction suppresses the ability of gremlin to induce the activation of intracellular signaling pathways in ECs, including ERK_{1/2} and p38 mitogen-activated protein kinase phosphorylation. Also, it inhibits EC

chemotactic migration, sprouting, and motility, all activities that are mediated by a productive interaction of gremlin with VEGFR2.²⁹

NRP-1 is a transmembrane glycoprotein involved in the interaction with a plethora of binding partners, including class-3 semaphorin receptors, heparin-binding growth factors, and HSPGs.⁵¹ Also, NRP-1 core protein is modified with either a single HS or chondroitin sulfate chain depending on the expressing cell type, thus increasing the complexity of NRP-1 extracellular interactions.⁵² Several sets of experimental evidence indicate that the binding of mammalian heparin-binding VEGF isoforms to HS and NRP-1 is interdependent.⁴ Gremlin does not contain the amino acid sequence CDKPRR present in the VEGF-A165 carboxyl terminus and involved in the interaction with b1b2 ectodomains of the NRP-1 core protein.⁵³ Even though we cannot rule out the possibility that gremlin may bind the HS chain of NRP-1 in target cells, our data indicate that, at variance with VEGF-A165, gremlin does not interact with recombinant NRP-1 and does not trigger the formation of a VEGFR2/NRP-1 complex in ECs. Also, the structural bases for heparin/HS interaction may differ between VEGF isoforms and gremlin. Indeed, VEGFs bind HS via a highly basic carboxyl-terminal region distinct from the cystine-knot domain of the protein and encoded by alternatively spliced exons.⁴ At variance, gremlin may interact with heparin/HS via a linear basic patch along the third loop of its cystine-knot domain, as suggested by homology modeling prediction studies based on the cystine-knot BMP antagonist sclerostin.^{31,32} Thus, gremlin differs from canonical heparin-binding VEGFs in the ability to co-opt VEGFR2 coreceptors and appears to exert a VEGFR2-dependent proangiogenic activation of ECs with mechanisms that are, at least in part, different from VEGFs. For instance, HSPGs contribute to VEGF-triggered angiogenesis by a mechanism dependent on the modulation of $\alpha_6\beta_1$ integrin expression on the EC surface.⁵⁴ At variance with VEGF-A, gremlin does not upregulate the expression of α_6 integrin in ECs (data not shown), further underscoring the different mechanism of action of the 2 angiogenic factors.

Chemical or enzymatic modifications of the *E. coli* capsular K5 polysaccharide allow the production of "biotechnological" semisynthetic heparin/HS-like compounds with selected chemical features, with potential implications in the therapy of various human pathologies, including thromboembolic diseases, viral infection, and neoplasia.^{16,55} Here we evaluated the gremlin-binding capacity of a series of specific *N*-, *O*-, or *N,O*-sulfated nonanticoagulant K5 derivatives.³³ Among the compounds tested, highly sulfated K5-N,OS(H) binds gremlin with higher affinity compared with the corresponding derivative K5-OS(H) devoid of sulfate group in the *N* position but bearing an identical total negative charge ($\text{SO}_3^-/\text{COO}^-$ of 3.8 for both compounds³³). K5-OS(H) consists of the virtually homogeneous repeat of $\text{GlcA}2,3\text{SO}_3^- - \text{GlcNAc}3,6\text{SO}_3^-$ disaccharide units, whereas most of K5-N,OS(H) sequences are represented by $\text{GlcA}2,3\text{SO}_3^- - \text{GlcNSO}_3^-,6\text{SO}_3^-$ disaccharide units.³³ Our data indicate that the requirement for *N*-sulfation present in K5-N,OS(H) cannot be fully overcome by the high density charge present in the highly *O*-sulfated K5-OS(H). Similarly, low sulfated K5-N,OS(L) binds gremlin more efficiently than

K5-OS(L), even though both compounds have a $\text{SO}_3^-/\text{COO}^-$ value of 1.7.³³ On the other hand, K5-NS devoid of sulfate groups in *O* positions ($\text{SO}_3^-/\text{COO}^-$ of 1.0) does not have a significant interaction with gremlin. Thus, in agreement with the results obtained with selectively desulfated heparins, *N*- and *O*-sulfate groups are required for gremlin interaction with sulfated K5 derivatives.

Gremlin exerts both BMP-dependent and BMP-independent functions in different physiopathological conditions by inhibiting BMP-mediated TGF- β receptor activation or by a direct activation of VEGFR2 signaling, respectively. In this respect, it is interesting to note that a complex, not yet fully elucidated cross-talk may exist among TGF- β /BMP, VEGFR2, and canonical and noncanonical Wingless (Wnt) signaling pathways during angiogenesis,⁵⁶ making unpredictable the impact of the modulation of a single agonist/antagonist on the neovascularization process in different pathological conditions. Here, we demonstrate that K5-N,OS(H) is a potent antagonist of gremlin, inhibiting VEGFR2 interaction and angiogenic activity *in vitro* and *in vivo*. Also, K5-N,OS(H) may prevent gremlin-driven tumor neovascularization, as indicated by its capacity to suppress the angiogenic potential of gremlin-overexpressing human tumor PANC-1 cells in an *ex vivo* human artery ring assay. Previous observations had shown the ability of K5-N,OS(H) to inhibit the angiogenic activity of the heparin-binding molecules fibroblast growth factor-2 and HIV-1 Tat protein¹⁶ and to reduce tumor invasion by hampering heparanase activity¹⁶ and tumor metastasis.⁵⁷ Thus, K5-N,OS(H) may represent the basis for the design of novel nonanticoagulant biotechnological heparins endowed with a multitarget antineoplastic action by interacting with different angiogenic growth factors and limiting tumor cell invasion and metastasis. Also, preclinical and clinical studies identify gremlin as a potential therapeutic target in human fibrotic diseases characterized by alterations of TGF- β /BMP signaling and vascular defects in different organs as liver,⁵⁸ kidney,²⁴ and lung.²³ Given the role of gremlin in physiological development and different pathological conditions, additional preclinical *in vivo* studies will be required to define the therapeutic capability and possible side effects of gremlin antagonists, including K5-N,OS(H) and its derivatives.

Acknowledgments

We thank Dr Sara Lovecchio for contributions to the experiments and Dr Stefano Calza for statistical analysis.

Sources of Funding

This work was supported by grants from Ministero dell'Istruzione, dell'Università e della Ricerca (MIUR), Associazione Italiana per la Ricerca sul Cancro (AIRC) (Grant 10396), Fondazione Berlucci, CARIPLO (Grant 2008-2264 and the NOBEL Project) (to M.P.); from MIUR, Istituto Superiore di Sanità (AIDS Project Grant 40H.51), and CARIPLO (Grant 2008-2198) (to M.R.); and from MIUR and My First AIRC Grant 9161 (to S.M.). Dr Ravelli was supported by a Fondazione Italiana per la Ricerca sul Cancro fellowship.

Disclosures

None.

References

- Carmeliet P, Jain RK. Angiogenesis in cancer and other diseases. *Nature*. 2000;407:249–257.
- Yancopoulos GD, Davis S, Gale NW, Rudge JS, Wiegand SJ, Holash J. Vascular-specific growth factors and blood vessel formation. *Nature*. 2000;407:242–248.
- Neufeld G, Cohen T, Gengrinovitch S, Poltorak Z. Vascular endothelial growth factor (VEGF) and its receptors. *FASEB J*. 1999;13:9–22.
- Grunewald FS, Protá AE, Giese A, Ballmer-Hofer K. Structure-function analysis of VEGF receptor activation and the role of coreceptors in angiogenic signaling. *Biochim Biophys Acta*. 2010;1804:567–580.
- Krilleke D, DeErkenez A, Schubert W, Giri I, Robinson GS, Ng YS, Shima DT. Molecular mapping and functional characterization of the VEGF164 heparin-binding domain. *J Biol Chem*. 2007;282:28045–28056.
- Lindahl U. Heparan sulfate-protein interactions: a concept for drug design? *Thromb Haemost*. 2007;98:109–115.
- Iozzo RV, San Antonio JD. Heparan sulfate proteoglycans: heavy hitters in the angiogenesis arena. *J Clin Invest*. 2001;108:349–355.
- Houck KA, Leung DW, Rowland AM, Winer J, Ferrara N. Dual regulation of vascular endothelial growth factor bioavailability by genetic and proteolytic mechanisms. *J Biol Chem*. 1992;267:26031–26037.
- Kawamura H, Li X, Goishi K, van Meeteren LA, Jakobsson L, Cebe-Suarez S, Shimizu A, Edholm D, Ballmer-Hofer K, Kjellen L, Klagsbrun M, Claesson-Welsh L. Neuropilin-1 in regulation of VEGF-induced activation of p38MAPK and endothelial cell organization. *Blood*. 2008;112:3638–3649.
- Robinson CJ, Mulloy B, Gallagher JT, Stringer SE. VEGF165-binding sites within heparan sulfate encompass two highly sulfated domains and can be liberated by K5 lyase. *J Biol Chem*. 2006;281:1731–1740.
- Maccarana M, Casu B, Lindahl U. Minimal sequence in heparin/heparan sulfate required for binding of basic fibroblast growth factor. *J Biol Chem*. 1994;269:3903–3903.
- Guimond S, Maccarana M, Olwin BB, Lindahl U, Rapraeger AC. Activating and inhibitory heparin sequences for FGF-2 (basic FGF). Distinct requirements for FGF-1, FGF-2, and FGF-4. *J Biol Chem*. 1993;268:23906–23914.
- Rusnati M, Urbinati C. Polysulfated/sulfonated compounds for the development of drugs at the crossroad of viral infection and oncogenesis. *Curr Pharm Des*. 2009;15:2946–2957.
- Presta M, Leali D, Stabile H, Ronca R, Camozzi M, Coco L, Moroni E, Liekens S, Rusnati M. Heparin derivatives as angiogenesis inhibitors. *Curr Pharm Des*. 2003;9:553–566.
- Presta M, Oreste P, Zoppetti G, Belleri M, Tanghetti E, Leali D, Urbinati C, Bugatti A, Ronca R, Nicoli S, Moroni E, Stabile H, Camozzi M, Hernandez GA, Mitola S, Dell'Era P, Rusnati M, Ribatti D. Antiangiogenic activity of semisynthetic biotechnological heparins: low-molecular-weight-sulfated *Escherichia coli* K5 polysaccharide derivatives as fibroblast growth factor antagonists. *Arterioscler Thromb Vasc Biol*. 2005;25:71–76.
- Rusnati M, Oreste P, Zoppetti G, Presta M. Biotechnological engineering of heparin/heparan sulphate: a novel area of multi-target drug discovery. *Curr Pharm Des*. 2005;11:2489–2499.
- Pearce JJ, Penny G, Rossant J. A mouse cerberus/Dan-related gene family. *Dev Biol*. 1999;209:98–110.
- Vitt UA, Hsu SY, Hsueh AJ. Evolution and classification of cystine knot-containing hormones and related extracellular signaling molecules. *Mol Endocrinol*. 2001;15:681–694.
- Balemans W, Van Hul W. Extracellular regulation of BMP signaling in vertebrates: a cocktail of modulators. *Dev Biol*. 2002;250:231–250.
- Khokha MK, Hsu D, Brunet LJ, Dionne MS, Harland RM. Gremlin is the bmp antagonist required for maintenance of SHH and FGF signals during limb patterning. *Nat Genet*. 2003;34:303–307.
- Lu MM, Yang H, Zhang L, Shu W, Blair DG, Morrisey EE. The bone morphogenic protein antagonist gremlin regulates proximal-distal patterning of the lung. *Dev Dyn*. 2001;222:667–680.
- Michos O, Panman L, Vintersten K, Beier K, Zeller R, Zuniga A. Gremlin-mediated BMP antagonism induces the epithelial-mesenchymal feedback signaling controlling metanephric kidney and limb organogenesis. *Development*. 2004;131:3401–3410.
- Costello CM, Cahill E, Martin F, Gaine S, McLoughlin P. Role of gremlin in the lung: development and disease. *Am J Respir Cell Mol Biol*;42:517–523.

24. Lappin DW, McMahon R, Murphy M, Brady HR. Gremlin: an example of the re-emergence of developmental programmes in diabetic nephropathy. *Nephrol Dial Transplant*. 2002;17(suppl 9):65–67.
25. Namkoong H, Shin SM, Kim HK, Ha SA, Cho GW, Hur SY, Kim TE, Kim JW. The bone morphogenetic protein antagonist gremlin 1 is over-expressed in human cancers and interacts with YWHAH protein. *BMC Cancer*. 2006;6:74.
26. Sneddon JB, Zhen HH, Montgomery K, van de Rijn M, Tward AD, West R, Gladstone H, Chang HY, Morganroth GS, Oro AE, Brown PO. Bone morphogenetic protein antagonist gremlin 1 is widely expressed by cancer-associated stromal cells and can promote tumor cell proliferation. *Proc Natl Acad Sci U S A*. 2006;103:14842–14847.
27. Stabile H, Mitola S, Moroni E, Belleri M, Nicoli S, Coltrini D, Peri F, Pessi A, Orsatti L, Talamo F, Castronovo V, Waltregny D, Cotelli F, Ribatti D, Presta M. Bone morphogenetic protein antagonist Drm/gremlin is a novel proangiogenic factor. *Blood*. 2007;109:1834–1840.
28. Mitola S, Moroni E, Ravelli C, Andres G, Belleri M, Presta M. Angiopoietin-1 mediates the pro-angiogenic activity of the bone morphogenetic protein antagonist Drm. *Blood*. 2008;112:1154–1157.
29. Mitola S, Ravelli C, Moroni E, Salvi V, Leali D, Ballmer-Hofer K, Zammataro L, Presta M. Gremlin is a novel agonist of the major proangiogenic receptor VEGFR2. *Blood*. 2010;116:3677–3680.
30. Topol LZ, Bardot B, Zhang Q, Resau J, Huillard E, Marx M, Calothy G, Blair DG. Biosynthesis, post-translation modification, and functional characterization of Drm/gremlin. *J Biol Chem*. 2000;275:8785–8793.
31. Veverka V, Henry AJ, Slocombe PM, Ventom A, Mulloy B, Muskett FW, Muzylak M, Greenslade K, Moore A, Zhang L, Gong J, Qian X, Paszty C, Taylor RJ, Robinson MK, Carr MD. Characterization of the structural features and interactions of sclerostin: molecular insight into a key regulator of Wnt-mediated bone formation. *J Biol Chem*. 2009;284:10890–10900.
32. Rider CC, Mulloy B. Bone morphogenetic protein and growth differentiation factor cytokine families and their protein antagonists. *Biochem J*. 2010;429:1–12.
33. Leali D, Belleri M, Urbinati C, Coltrini D, Oreste P, Zoppetti G, Ribatti D, Rusnati M, Presta M. Fibroblast growth factor-2 antagonist activity and angiostatic capacity of sulfated *Escherichia coli* K5 polysaccharide derivatives. *J Biol Chem*. 2001;276:37900–37908.
34. Rusnati M, Coltrini D, Oreste P, Zoppetti G, Albini A, Noonan D, d'Adda di Fagagna F, Giacca M, Presta M. Interaction of HIV-1 Tat protein with heparin: role of the backbone structure, sulfation, and size. *J Biol Chem*. 1997;272:11313–11320.
35. Zhang Z, Coomans C, David G. Membrane heparan sulfate proteoglycan-supported FGF2-FGFR1 signaling: evidence in support of the “cooperative end structures” model. *J Biol Chem*. 2001;276:41921–41929.
36. Rusnati M, Urbinati C, Caputo A, Possati L, Lortat-Jacob H, Giacca M, Ribatti D, Presta M. Pentosan polysulfate as an inhibitor of extracellular HIV-1 Tat. *J Biol Chem*. 2001;276:22420–22425.
37. Grinspan JB, Mueller SN, Levine EM. Bovine endothelial cells transformed in vitro by benzo(a)pyrene. *J Cell Physiol*. 1983;114:328–338.
38. Esko JD. Genetic analysis of proteoglycan structure, function and metabolism. *Curr Opin Cell Biol*. 1991;3:805–816.
39. Safaiyan F, Kolset SO, Prydz K, Gottfridsson E, Lindahl U, Salmivirta M. Selective effects of sodium chlorate treatment on the sulfation of heparan sulfate. *J Biol Chem*. 1999;274:36267–36273.
40. De Palma M, Naldini L. Transduction of a gene expression cassette using advanced generation lentiviral vectors. *Methods Enzymol*. 2002;346:514–529.
41. Rusnati M, Urbinati C, Presta M. Internalization of basic fibroblast growth factor (bFGF) in cultured endothelial cells: role of the low affinity heparin-like bFGF receptors. *J Cell Physiol*. 1993;154:152–161.
42. Margosio B, Marchetti D, Vergani V, Giavazzi R, Rusnati M, Presta M, Taraboletti G. Thrombospondin 1 as a scavenger for matrix-associated fibroblast growth factor 2. *Blood*. 2003;102:4399–4406.
43. Hothorn T, Bretz F, Westfall P. Simultaneous inference in general parametric models. *Biom J*. 2008;50:346–363.
44. Mousa SA, Petersen LJ. Anti-cancer properties of low-molecular-weight heparin: preclinical evidence. *Thromb Haemost*. 2009;102:258–267.
45. Rostand KS, Esko JD. Microbial adherence to and invasion through proteoglycans. *Infect Immun*. 1997;65:1–8.
46. Gitay-Goren H, Soker S, Vlodavsky I, Neufeld G. The binding of vascular endothelial growth factor to its receptors is dependent on cell surface-associated heparin-like molecules. *J Biol Chem*. 1992;267:6093–6098.
47. Cohen T, Gitay-Goren H, Sharon R, Shibuya M, Halaban R, Levi BZ, Neufeld G. VEGF121, a vascular endothelial growth factor (VEGF) isoform lacking heparin binding ability, requires cell-surface heparan sulfates for efficient binding to the VEGF receptors of human melanoma cells. *J Biol Chem*. 1995;270:11322–11326.
48. Casu B, Grazioli G, Razi N, Guerrini M, Naggi A, Torri G, Oreste P, Tursi F, Zoppetti G, Lindahl U. Heparin-like compounds prepared by chemical modification of capsular polysaccharide from *E. coli* K5. *Carbohydr Res*. 1994;263:271–284.
49. Esko JD, Lindahl U. Molecular diversity of heparan sulfate. *J Clin Invest*. 2001;108:169–173.
50. Ono K, Hattori H, Takeshita S, Kurita A, Ishihara M. Structural features in heparin that interact with VEGF165 and modulate its biological activity. *Glycobiology*. 1999;9:705–711.
51. Pellet-Manly C, Frankel P, Jia H, Zachary I. Neuropilins: structure, function and role in disease. *Biochem J*. 2008;411:211–226.
52. Shintani Y, Takashima S, Asano Y, Kato H, Liao Y, Yamazaki S, Tsukamoto O, Seguchi O, Yamamoto H, Fukushima T, Sugahara K, Kitakaze M, Hori M. Glycosaminoglycan modification of neuropilin-1 modulates VEGFR2 signaling. *EMBO J*. 2006;25:3045–3055.
53. Geretti E, Klagsbrun M. Neuropilins: novel targets for anti-angiogenesis therapies. *Cell Adh Migr*. 2007;1:56–61.
54. Lee TH, Seng S, Li H, Kennel SJ, Avraham HK, Avraham S. Integrin regulation by vascular endothelial growth factor in human brain microvascular endothelial cells: role of $\alpha 6 \beta 1$ integrin in angiogenesis. *J Biol Chem*. 2006;281:40450–40460.
55. Rusnati M, Vicenzi E, Donalisio M, Oreste P, Landolfo S, Lembo D. Sulfated K5 *Escherichia coli* polysaccharide derivatives: a novel class of candidate antiviral microbicides. *Pharmacol Ther*. 2009;123:310–322.
56. Goodwin AM, D'Amore PA. Wnt signaling in the vasculature. *Angiogenesis*. 2002;5:1–9.
57. Poggi A, Rossi C, Casella N, Bruno C, Sturiale L, Dossi C, Naggi A. Inhibition of b16-bl6 melanoma lung colonies by semisynthetic sulfaminoheparosan sulfates from *E. coli* K5 polysaccharide. *Semin Thromb Hemost*. 2002;28:383–392.
58. Boers W, Aarass S, Linthorst C, Pinzani M, Elferink RO, Bosma P. Transcriptional profiling reveals novel markers of liver fibrogenesis: gremlin and insulin-like growth factor-binding proteins. *J Biol Chem*. 2006;281:16289–16295.